Available online at www.sciencedirect.com
ScienceDirect
Catalysis Today 132 (2008) 2–8
CATALYSIS TODAY
www.elsevier.com/locate/cattod

Nano-structuring of complex metal oxides for catalytic oxidation

Wataru Ueda *, Masahiro Sadakane, Hitoshi Ogihara

Catalysis Research Center, Hokkaido University, N21-W10, Kita-ku, Sapporo 001-0021, Japan

Available online 31 January 2008

Abstract

New crystalline solid materials of Mo_3VO_x having high-dimensional structures were synthesized in a single crystalline form using a hydrothermal method where the essential structural unit in the structure already presents in the preparative solution and the fundamental structure of Mo_3VO_x is formed as a result of self-organization between negatively charged pentagonal units and VO^{2+} cations. We also synthesized metal oxides by using organic solids with particular shapes as templates in order to create nano-macrostructures. Three-dimensionally ordered macroporous (3DOM) materials of polycrystalline spinel- and perovskite-type materials were fabricated using a colloidal crystal template method in extremely high yield. In the synthesis of oxide nanotubes, we demonstrate that various oxide nanotubes could be synthesized by the adsorption and hydrolysis of precursors on the surface of carbon nanofiber templates and by the oxidative removal of templates. A variety of oxide nanotubes such as thick, thin, and helical nanotubes reflecting the shapes of carbon nanofibers could be synthesized.

Keywords: Complex metal oxide catalyst; Nano-sized structure; Unit synthesis; Soft synthesis; Template

1. Introduction

Solid-state materials with nano-scale structures are expected to be potential catalysts for chemical reactions because the materials would have attractive catalytic properties due to their unique reaction field around catalytic active sites. In addition, three-dimensional organization of catalytic components is highly important for solid-state catalysts, particularly for a multi-functional one which is often necessary for various multi-steps catalytic reactions like catalytic selective oxidations. Therefore, it appeared that nano-scale materials structuring using inorganic soft syntheses like sol–gel method, hydrothermal method, solvothermal method, organic template method, and so on, thought to be significantly important.

In this summary report the following three types of nano-structuring methods for complex metal oxide catalysts: (i) unit synthesis method for preparing crystalline materials with high-dimensional crystal structures, (ii) organic sphere template method for three-dimensionally ordered macroporous (3DOM) materials preparation, and (iii) carbon nanofiber template method for nanotube-shaped materials are described.

2. Unit synthesis for preparing crystalline Mo_3VO_x catalysts with high-dimensional structures

Many of the catalysts for selective oxidation are composed of metal oxides like molybdenum and vanadium oxide as key elements [1]. The most common preparation method of these catalysts is so-called ‘‘mixed-and baked’’ method, where starting materials in states of metal oxides or metal salts are mixed either in a solid-state or in a solution (mixed) and then the mixture is calcined (baked) to be metal oxides. This method is easy and convenient for a large-scale preparation. However, precise controls of crystal structure, elemental composition in the structure, particle shape, surface area, and so forth, which often affect catalytic performance dramatically, are usually very difficult to be conducted under control, mainly because high-temperature heat-process is generally unpredictable for complicated metal oxide systems.

Recently, much attention has been attracted to an orthorhombic MoVTe(Sb)NbO mixed metal oxide catalyst which is typically recognized as a complicated system [2–4]. The catalyst has high activities for the ammoxidation of propane and achieves 50–60% acrylonitrile yield at relatively low reaction temperature. This complex mixed metal oxide assumes a layered (orthorhombic) structure with slabs consisting of 6-membered ring and 7-membered ring units

* Corresponding author.
E-mail address: ueda@cat.hokudai.ac.jp (W. Ueda).

0920-5861/$ – see front matter © 2007 Elsevier B.V. All rights reserved.
doi:10.1016/j.cattod.2007.12.012

with MO_6 octahedra and pentagonal $\{(M)M_5O_{27}\}$ unit with a MO_7 pentagonal bipyramid and five edge-sharing MO_6 octahedra. There are four pentagonal units with 6-membered ring and 7-membered ring in the unit cell, that is, in the case, isotypic with Cu–Nb–O–X (X = Cl, Br, and I) and Cs–Nb–W–O system [5–8]. The main components are Mo and V, and Nb, and Te (or Sb) exist as minor elements.

Unlike other simple Mo–based metal oxides, the Mo–V–O based catalysts are so complicated that it is not easy to prepare simply by solid-state preparation methods. In fact, careful preparation (metal ratio, concentration and pH of the initial mixture, calcination temperature, calcination atmosphere, etc.) is inevitably necessary. In order to obtain such complicated structural material, we have tried to develop a new synthetic procedure. Our approach is to use hydrothermal reaction which is believed to be profitable for meta-stable materials. Recently, we have succeeded in synthesizing orthorhombic mixed metal oxides containing Mo and V without other elements (Te, Sb, or Nb) in pure form [9–13]. On the basis of the various preparative effects, we can shed light on the formation mechanism of the Mo–V based materials.

Here in this section, we describe our recent achievement of the preparation of orthorhombic and a novel trigonal Mo_3VO_x oxide, both of which contain the same building units, 6-member rings and 7-member rings and pentagonal unit with different ratio. Both of the orthorhombic and the trigonal Mo_3VO_x are found to show an outstanding catalytic performance for acrolein selective oxidation, thus revealing the importance of these structures for the catalytic oxidation activity.

The orthorhombic and trigonal Mo_3VO_x mixed metal oxides were synthesized from a reaction mixture of ammonium heptamolybdate $(NH_4)_6Mo_7O_{24}{\cdot}4H_2O$ and vanadyl sulfate $VOSO_4{\cdot}nH_2O$ (Mo 50 mmol and 12.5 mmol) in H_2O (240 mL) under hydrothermal condition. By controlling pH of the precursor solution, the orthorhombic (pH 3.2) or trigonal (pH 2.2) Mo_3VO_x could be separately synthesized. The crude materials usually contained an amorphous phase as a byproduct in a small amount, but it could be removed by washing with an aqueous solution of oxalic acid. Metal compositions of Mo/V were determined by ICP-AES to be ca. 3 for the both materials.

Fundamental structures of the orthorhombic and trigonal Mo_3VO_x were constructed on the basis of the TEM images of the samples, as shown in Fig. 1 which represents structures along the [0 0 1] zone axis of the orthorhombic and trigonal Mo_3VO_x. The pentagonal unit was placed in a position surrounded by three 7-membered rings and two 6-membered rings but in different manner from the orthorhombic one to the trigonal one as presented in Fig. 1. Both structures were confirmed by refining the powder XRD data by Rietveld method. The XRD patterns of the structures were well-simulated with lattice parameter (see numerical data in Fig. 1) and reasonably converged. As the Rietveld refinement using other deduced models never converged, the proposed structures came to be almost confirmed.

The orthorhombic or trigonal Mo_3VO_x were synthesized from the dark violet solution which was immediately formed by mixing the aqueous solutions of ammonium heptamolybdate and vanadyl sulfate at room temperature. We measured Raman spectra of this precursor solution before the hydrothermal reaction and also of polyoxomolybdate solutions containing $Mo_{72}V_{30}$ [14], Mo_{132} [15], or $Mo_{57}V_6$ [16], all of which are composed of pentagonal $\{(Mo)Mo_5\}$ units in their cluster. The

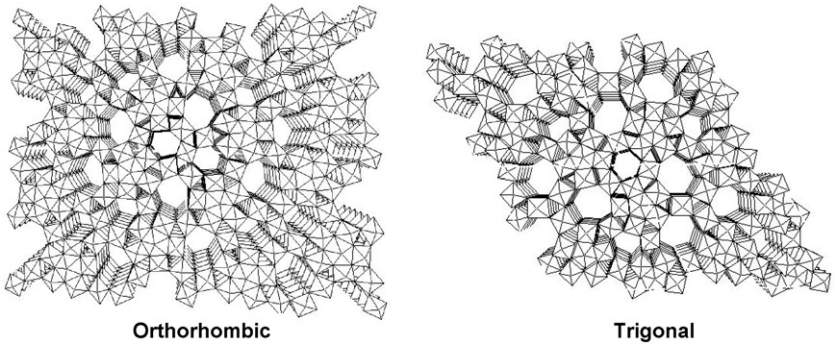

Fig. 1. Crystal structures of orthorhombic and trigonal Mo_3VO_x and their crystal data.Crystallographic data

	Composition	
	$Mo_1V_{0.34}O_{3.58}$	$Mo_1V_{0.33}O_{3.43}$
Crystal system	Orthorhombic	Trigonal
Space group	Pba2 (No. 32)	P3 (No. 143)
Z	4	1
a (Å)	21.085(10)	21.433(3)
b (Å)	26.556(13)	
c (Å)	3.9974(17)	4.0045(18)
V (Å^3)	2238.3(18)	1593.8(3)
R_{wp}	13.76	12.23
R_e	6.67	4.95
S	2.06	2.47

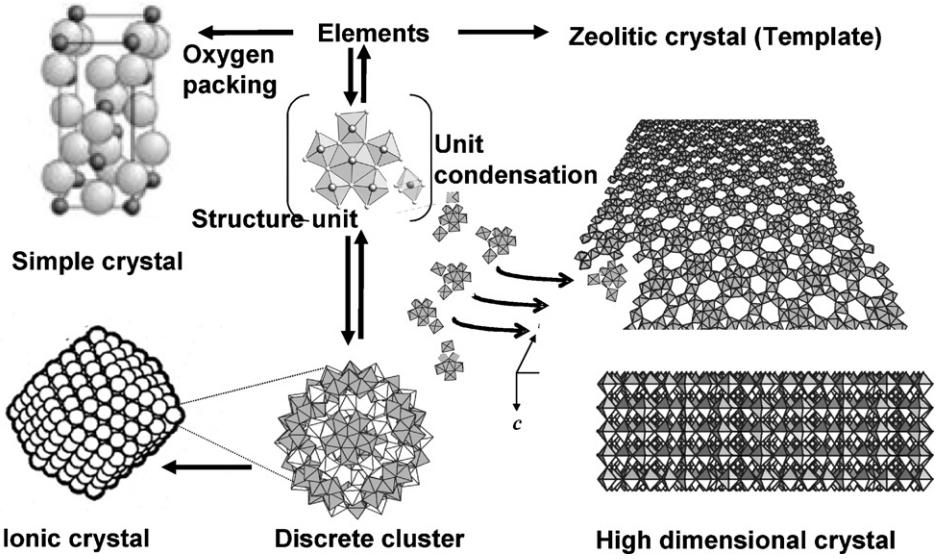

Fig. 2. Various formation processes of metal oxides.

characteristic Raman peaks were observed at 1000–700 cm^{-1} not only for the precursor solution but also for all polyoxomolybdate solutions. This coincident clearly suggests that the pentagonal {(Mo)Mo_5} unit is present in the precursor solution even before the hydrothermal reaction. This was confirmed by UV–vis analyses as well. By analogy of that the discrete polyoxomolybdate clusters have been prepared from room temperature to 363 K by a reaction of the pentagonal units with molybdenum and other metal species, it is likely that the pentagonal unit formed in the precursor solution gradually reacts with other molybdenum and vanadium and condensate together forming three-dimensional Mo_3VO_x solid with the orthorhombic or trigonal structures under the hydrothermal reaction condition, as illustrated in the right part of Fig. 2. The process that gives such high-dimensional solid-state materials is completely different form others in which typical complex metal oxides form under the control of oxygen anion packing, ionic interaction of polymeric clusters, and template effect for zeolitic materials (the left part of Fig. 2).

We noticed that the formation of the orthorhombic or trigonal Mo_3VO_x depends on the pH in the precursor solution. The pH is also known to be one of the most important factors to produce the various polyoxomolybdate [17]. We think that this is also an evident that proofs the unit condensation during the hydrothermal reaction because higher pH condition tends to give more condensed units, like from unit condensate of two pentagonal units to three units. Then this ultimately controls the final solid phase, the orthorhombic, trigonal, or others which is not known yet.

The trigonal Mo_3VO_x catalyst has the outstanding catalytic performance for oxidation of acrolein to acylic acid, and the conversion of acrolein was achieved to almost 100% at 463 K and the selectivity to acrylic acid was more than 90% (the yield 90%). The orthorhombic Mo_3VO_x catalyst showed a similar high catalytic performance. It is noteworthy that these catalytic activities are significantly superior to that of Mo–V based oxide catalysts commercially used, which required much higher temperature, usually more than 500 K in order to attain performance. These results indicate that the trigonal and/or orthorhombic Mo_3VO_x phases are potentially true catalytic active species in the previously reported Mo–V based catalyst. In addition we have to emphasize that these materials can be realized by nano-level control in catalyst preparation.

3. Organic sphere template method for three-dimensionally ordered macroporous (3DOM) materials preparation

Fabrication of ordered materials in nano-scale order has been one of the most important topics in recent years, and three-dimensionally ordered macroporous (3DOM) materials with pores sized in the sub-micrometer range have become the focus of studies because of their application in photonic crystals, catalysis, and separation [18]. To date almost all of the 3DOM metal oxides have been synthesized by alkoxide-based sol–gel processes: (i) a colloidal crystal template which is prepared by ordering mono-disperse spheres, e.g., polystyrene, poly-(methyl methacrylate), or silica, into a face-centered close-packed array (opal structure); (ii) interstices in the colloidal crystal are then filled with liquid-state metal species, either neat or in solution, which solidify in situ via a sol–gel transformation, resulting in an intermediate composite structure; (iii) an ordered foam is produced after removing the template by calcinations or extraction.

The ordered (‘‘inverse opals’’) structures synthesized using this method consist of a skeleton surrounding of uniform close-packed macropores. The macropores are interconnected through windows that form as a result of the contact between the template spheres prior to the infiltration of the precursor solution. However, the alkoxide-based sol–gel method can be applied only to the synthesis of metal oxides (generally, Si, Ti, Zr, and mixture of these), if the metal alkoxide precursor is only moderately reactive. Most of the other metal alkoxides react so quickly that the reaction cannot be controlled. Another problem

is that commercially available salts of these metals are usually not suitable for starting materials because of their melting temperature. These salts melt at a temperature where the template polymer decomposes and, therefore, do not form the 3DOM structure. Solidification of the transition and lanthanide metal elements before decomposition of the polymer template are, therefore, very important.

An elegant method for producing 3DOM materials of the transition-metal oxides has been reported by Stein et al. [19]. They infiltrated metal salts (acetate or nitrate) into voids of the colloidal crystals and solidified them as oxalate salts by reacting with oxalic acid. Solidification by reacting base, like ammonia [20] or EDTA [21] has also been reported. These methods are, however, not suitable for the preparation of 3DOM materials when mixed metal oxides because metal species has a different reactivity with oxalic acid or base, and the produced oxalate salts or metal hydroxides have different solubility in the reacting media, which causes a mixed metal oxide with an undesired metal ratio [22].

Synthetic procedures that ensure the chemical homogeneity of the product are highly needed. 3DOM $Sm_{0.5}Sr_{0.5}CoO_3$ has been prepared from mixed nitrate salts. This is the only example where no solidification is needed [23]. Hur et al. have prepared 3DOM $La_{0.7}Ca_{0.3-x}Sr_xMnO_3$ type perovskite compounds from a mixed metal alkoxide precursor, which is pre-synthesized by reacting their acetate salts with 2-methoxyethanol under acidic conditions [24]. Our strategy is to use an ethylene glycol (EG)–methanol mixed solution of metal nitrate salts, which are converted to a mixed metal glyoxylate salt by in situ nitrate oxidation at low temperature before the template is removed. Calcination removes the polymer template and provides the conversion of the glyoxylate salt into the mixed metal oxide, i.e., 3DOM perovskite-type materials. We have reported the preparation of well-ordered 3DOM mixed iron oxides in high yield by our method [25–28]. We here describe the method, structural characterization, and formation mechanism of the well-ordered 3DOM spinel-type polycrystalline mixed iron oxide MFe_2O_4 (M: Ni, Zn, and Co) with a skeleton structure in detail.

Typical procedure is following: metal nitrates mixture (total metal concentration: 2 M) was dissolved with ca. 8 mL of ethylene glycol (EG) by stirring in a 100 mL beaker at room temperature for 2 h, and the produced EG solution was poured into a 25 mL volumetric flask. Methanol (8 mL, 32 vol%) and EG were added in amounts necessary to achieve the desired concentration. Then, PMMA colloidal crystals were soaked in the solution for 2 h. Excess solution was removed from the impregnated PMMA colloidal crystals by vacuum filtration. The obtained sample was allowed to dry in air at room temperature overnight. A 0.5 g amount of the sample was mixed with 2.5 g of quartz sands (10–15 mesh) and calcined in a tubular furnace (inner diameter ca. 22 mm) in an air flow (50 mL min^{-1}). The temperature was raised at a rate of 1 K min^{-1} to 873 K and held for 5 h.

Spinel formation was confirmed by XRD patterns and any by-products as metal oxides (NiO, ZnO, CoO, Co_3O_4, or iron oxide) could not be observed, indicating that homogeneous distribution of metal ions could be kept using this procedure. Their SEM images showed that well-ordered 3DOM structure was obtained in MFe_2O_4 (M = Ni, Zn, and Co) but not in $CuFe_2O_4$. $CuFe_2O_4$ is tetragonal with large difference between *a* and *c* lattice parameters, so that anisotropic crystal growth destroyed the 3DOM structure. On the other hand, MFe_2O_4 (M = Ni, Zn, and Co) are cubic and the crystals grow isotropically and gave 3DOM, suggesting that isotropic nature could be important to construct the 3DOM structure.

The inverse opal structures were classified into three structures, ''residual volume structure'', ''shell structure'', and ''skeleton structure'' [18]. The residual volume structure is inverse opal structure which can be produced when the whole space among the opal spheres is completely filled by the product materials. When the space is incompletely filled, the surface of the sphere templates is covered by the product materials, and the shell structure is generated. Most of amorphous compounds tend to form the shell structure. On the other hand, crystal compounds tend to form the skeleton structure.

The skeleton structure consists of struts-like bonds and vertexes, the struts connected two kinds of vertexes. The two vertexes are replicas of the former octahedral and tetrahedral voids of the opal structure. These struts and vertexes form a CaF_2 lattice, where 8-coordinated square prism calcium vertex is bigger than fluorine (the former tetrahedral voids of the opal) vertex. The model of the skeleton structure was depicted in Fig. 3. The view towards (1 1 1), (1 0 0), and (1 1 0) plane of the skeleton structure present hexagonal, square, and lozenge arrangement, respectively. As can be seen in Fig. 3, straight connections of the crystallites construct strut-like bonds, and agglomerations of the crystallites construct vertexes. The struts connect the tetragonal and square prism vertexes (marked as t and s, respectively, in Fig. 3) one after the other to produce inverse opal structure. Continuous ordering of the inverse opal structure was confirmed by observing the hexagonal, square, and lozenge arrangement of the (1 1 1) (in figure 3(d)), (1 0 0) (in figure 3(e)), and (1 1 0) planes. In the view toward (1 0 0) plane, long range order (ca. 3 μm long) of the small tetragonal vertexes and big square prism vertexes one after the other in the square arrangement could be observed. Average pore size of 183 ± 4 nm, which is a distance between the centers of two neighboring air spheres corresponds to 63% of shrinkage from the original PMMA sphere. This shrinkage was caused by melting of the PMMA spheres and sintering of the material.

Scheme 1 shows a possible formation mechanism. At the beginning, mixed metal nitrates react with EG to produce the mixed metal glyoxylate or oxalate salts in the void of the template spheres at a low temperature. Then the melting of PMMA during heating reduces the pore size and at the same time evaporation of methanol and remaining EG produces the air space in the void (shell structure). Further heating causes oxidative removal of the PMMA and convert the mixed metal glyoxylate derivatives to the desired spinel-type mixed oxides. Crystallite growth changes the 3DOM material from the ''shell structure'' to the ''skeleton structure''.

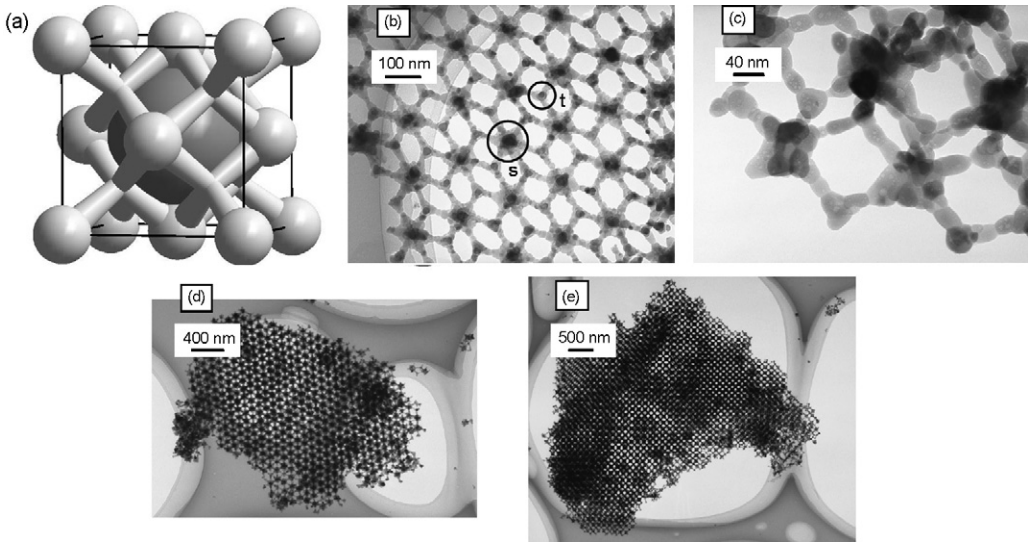

Fig. 3. Models of the inverse opals with skeleton structure (a) and TEM images (b–e) of 3DOM $ZnFe_2O_4$.

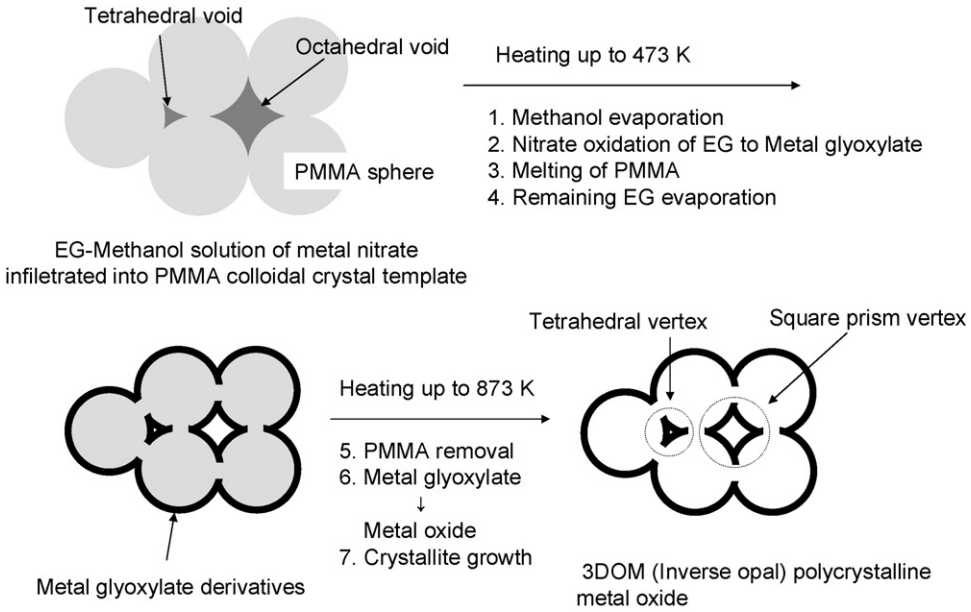

Scheme 1. Formation mechanism of 3DOM metal oxide.

4. Carbon nanofiber template method for nanotube-shaped materials

Since the discovery of carbon nanotubes, synthesis of nano-scale materials such as nanotubes, nanowires, nanoparticles, and nanoribbons have been extensively investigated. In particular, nanotubular materials have attracted increasing attention due to their specific mechanical, electrical, and chemical properties [29–31]. The template approach is a representative synthesis method for oxide nanotubes. Porous anodic alumina [32], organogels [33], hydrogels [34], cholesterol nanotubes [35], carbon nanotubes [36–38], and crystalline nanowires [39] have been used as templates. The advantage of template method is that shapes of formed nanotubes can be controlled by those of templates. There are, however, some difficulties in shape controlled synthesis of various oxide nanotubes; that is a limited template with various nano-scale structures. A simple shape-controllable synthesis of oxide nanotubes using carbon nanofibers as templates is highly desirable.

Recently, carbonaceous materials have been utilized as templates for the preparation of nano-scale materials. For example, mesoporous spheres of metal oxides and zeolite with unique supermicropores were synthesized using mesoporous carbons [40,41], and hollow metal oxide fibers with hierarchical architecture were synthesized using activated carbon fibers as templates [42]. Carbon nanofiber is well-known as one of the nano-scale carbonaceous materials [43]. A large amount of them can be produced by the decomposition of hydrocarbons or carbon monoxide over Ni, Co, or Fe catalysts. In addition, straight, bent, thin, and helical carbon nanofibers can be

produced by the control of reaction conditions [44–46]. If these carbon nanofibers with different shapes could be used as templates, metal oxide nanotubes with a variety of shape structures would be formed.

Here carbon nanofiber was used as a template [47]. The preparative procedure of oxide nanotube is following: The template was placed in a suction filtering unit and a precursor diluted with organic solvent (for example, $Zr(OnPr)_4$ (150 mM) in C_2H_5OH, $Al(OsecBu)_3$ (150 mM) in CCl_4, or $SiCl_4$ (500 mM) in CCl_4) was dropped into the carbon nanofiber template. Immediately after the precursor solution infiltrated into the space of the fibrous structure, excess precursor solution was removed by filtration. Obtained samples were dried in air at 393 K and the precursor adsorbed on the templates was immediately hydrolyzed by the water vapor in air. Consequently, the carbon nanofiber templates were covered with a thin oxide and hydroxide. This coating process was repeated 10–40 times. The carbon nanofiber templates were removed by the calcination in air at 1023 K for 4 h.

When we used a straight carbon nanofiber as templates with the size of 100 and 200 nm, the shapes of formed nanotubes were straight, and their inner diameters were ranged from ca. 100 to 200 nm. Wall thickness of ZrO_2 nanotube was ca. 30 nm, and that of Al_2O_3 and SiO_2 nanotubes was 10–20 nm. Wall thickness of nanotubes could be controlled by the number of coating processes. Also, it is considered that the wall of formed oxide nanotubes would thicken as the diameter of carbon nanofiber becomes larger.

When carbon nanofiber has a coiled structure, formed oxide nanotubes showed a helical structure, reflecting the shapes of carbon nanocoils with different coil diameters and pitches. Therefore, a variety of helical oxide nanotubes were formed and helical oxide nanotubes with various inner diameter, coil diameter, and coil pitches were observed. It was the first time that these helical ZrO_2, Al_2O_3, and SiO_2 nanotubes were synthesized. Until now, only organogels were used as templates for the synthesis of helical nanotubes, and helical SiO_2 and Ta_2O_5 nanotubes were obtained [46,48–52]. As for microtubes, TiO_2 microtubes were synthesized using carbon micro-coils as templates [53]. These facts suggest that the present method is promising and a variety of attractive nanotubular materials can be fabricated by using carbon nanofibers as templates. The present study also demonstrated that various oxide nanotubes could be synthesized by the adsorption and hydrolysis of precursors on the surface of carbon nanofiber templates only. This method is also applicable for the synthesis of nanotubes of complex metal oxides as demonstrated in Fig. 4 [54].

In the extension of the above method, we attempted the immobilization of nanofibrous metal oxide on the macrostructure materials. Silica fibers were used as macrostructured materials. First, a small amount of Ni particles which catalyze carbon nanofiber growth are supported on the silica fibers. After contacting methane over silica fiber-supported Ni (i.e., CVD process) carbon nanofiber was grown and immobilized on the silica fibers. The immobilized carbon nanofiber was used as templates for metal oxide nanotubes/nanofibers synthesis.

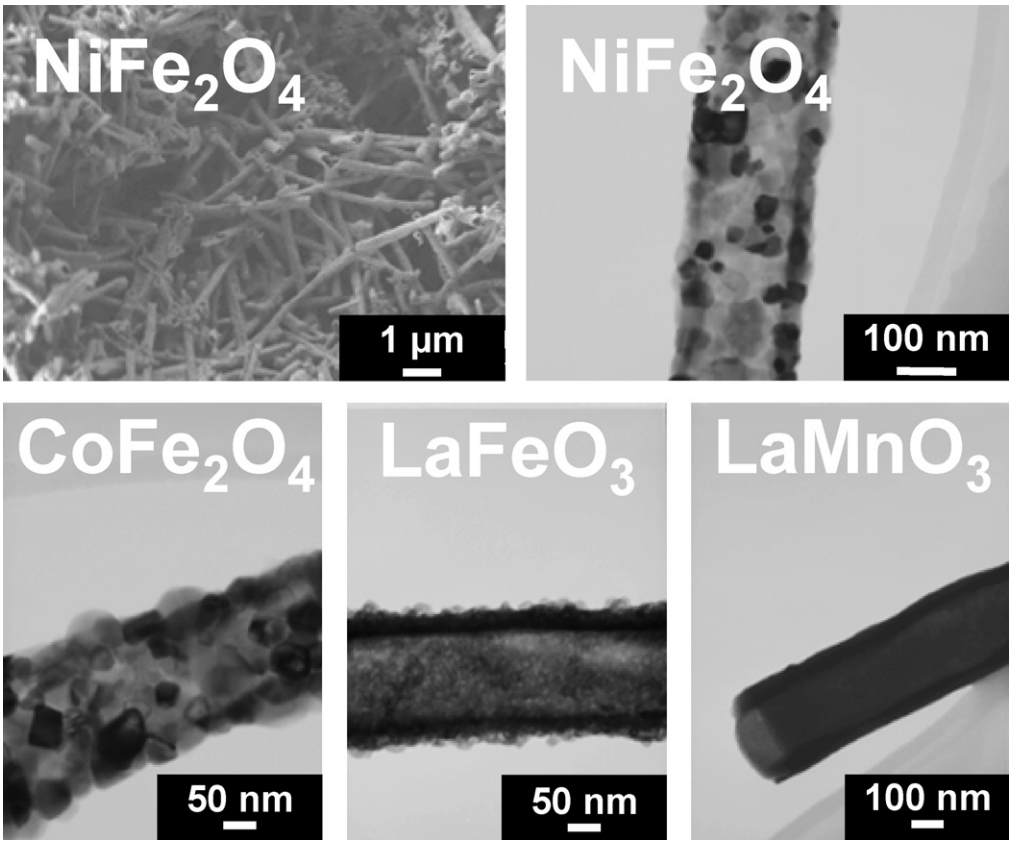

Fig. 4. Various nanotube-shaped complex metal oxides.

Eventually, the procedures produce silica fiber-immobilized metal oxide nanotubes/nanofibers.

5. Summary

We described three distinct methods for preparing mixed oxide catalysts with nano-stuctures in the size from atomic level to macro. These methods can provide multi-catalytic functions on the surface of mixed metal oxide which is highly important to accomplish high reaction selectivity and multi-step reactions. The methods also achieve the creation of uniform open spaces surrounded by catalytic surface in catalytic materials particles, which is obviously profitable for high catalytic performance. It is no doubt that nano-structuring and nano-fabrication of solid catalysts by the development of new catalyst preparation will bring new generation of solid-state catalysis.

References

[1] B.K. Hodnett, Heterogeneous Catalytic Oxidation, Wiley, New York, 2000.
[2] T. Ushikubo, K. Oshima, A. Kayou, M. Vaarkamp, M. Hatano, J. Catal. 169 (1997) 394.
[3] H. Tsuji, Y. Koyasu, J. Am. Chem. Soc. 124 (2002) 5608.
[4] H. Tsuji, K. Oshima, Y. Koyasu, Chem. Mater. 15 (2003) 2112.
[5] P. DeSanto Jr., D.J. Buttrey, R.K. Grasselli, C.G. Lugmair, A.F. Volpe Jr., B.H. Toby, T. Vogt, Z. Kristallogr. (2004) 219.
[6] P. DeSanto Jr., D.J. Buttrey, R.K. Grasselli, C.G. Lugmair, A.F. Volpe, B.H. Toby, T. Vogt, Top. Catal. 23 (2003) 23.
[7] R. Ross, B. Kratzheller, R. Gruehn, Z. Anorg. Allg. Chem. 587 (1990) 47.
[8] M. Lundberg, M. Sundberg, Ultramicroscopy 52 (1993) 429.
[9] M. Sadakane, N. Watanabe, T. Katou, Y. Nodasaka, W. Ueda, Angew. Chem. Int. Ed. 46 (2007) 1493.
[10] N. Watanabe, W. Ueda, Ind. Eng. Chem. Res. 45 (2006) 607.
[11] T. Katou, D. Vitry, W. Ueda, Catal. Today 91/92 (2004) 237.
[12] D. Vitry, Y. Morikawa, J.L. Dubois, W. Ueda, Appl. Catal. A 251 (2003) 411.
[13] T. Katou, D. Vitry, W. Ueda, Chem. Lett. 32 (2003) 1028.
[14] A. Mueller, A.M. Todea, J. Van Slageren, M. Dressel, H. Boegge, M. Schmidtmann, M. Luban, L. Engelhardt, M. Rusu, Angew. Chem. Int. Ed. 44 (2005) 3857.
[15] A. Mueller, E. Krichemeyer, H. Boegge, M. Schmidtmann, F. Peters, Angew. Chem. Int. Ed. 37 (1998) 3360.
[16] A. Mueller, E. Krichemeyer, S. Dillinger, H. Boegge, W. Plass, A. Proust, L. Dloczik, C. Meyer, R. Rohlfing, Z. Anorg. Allg. Chem. 620 (1994) 599.
[17] A. Mueller, P. Koegerler, A.W.M. Dress, Coord. Chem. Rev. 222 (2001) 193.
[18] R.C. Schroden, A. Stein, in: F. Caruso (Ed.), 3D Ordered Macroporous Material: Colloids and Colloid Assemblies, Wiley-VCH Verlag GmbH and Co. KGaA, Weinheim, Germany, 2004, p. 465.
[19] H. Yan, C.F. Blanford, B.T. Holland, W.H. Smyrl, A. Stein, Chem. Mater. 12 (2000) 1134.
[20] S. Sokolov, D. Bell, A. Stein, J. Am. Ceram. Soc. 86 (2003) 1481.
[21] Y. Zhang, Z. Lei, J. Li, S. Lu, New J. Chem. 25 (2001) 1118.
[22] H. Yan, C.F. Blanford, W.H. Smyrl, A. Stein, Chem. Commun. (2000) 1477.
[23] F. Chen, C. Xia, M. Liu, Chem. Lett. 1032 (2001).
[24] Y.N. Kim, S.J. Kim, E.K. Lee, E.O. Chi, N.H. Hur, C.S. Hong, J. Mater. Chem. 14 (2004) 1774.
[25] M. Sadakane, T. Asanuma, J. Kubo, W. Ueda, Chem. Mater. 17 (2005) 3546.
[26] M. Sadakane, C. Takahashi, N. Kato, T. Asanuma, H. Ogihara, W. Ueda, Chem. Lett. 35 (2006) 480.
[27] M. Sadakane, C. Takahashi, N. Kato, H. Ogihara, Y. Nodasaka, Y. Doi, Y. Hinatsu, W. Ueda, Bull. Chem. Soc. Jpn. 80 (2007) 677.
[28] M. Sadakane, T. Horiuchi, N. Kato, C. Takahashi, W. Ueda, Chem. Mater. 19 (2007) 5779.
[29] G.R. Patzke, F. Krumeich, R. Nesper, Angew. Chem. Ind. Ed. 41 (2002) 2446.
[30] Y. Xia, P. Yang, Y. Sun, Y. Wu, B. Mayers, B. Gates, Y. Yin, F. Kim, H. Yan, Adv. Mater. 15 (2003) 353.
[31] R.A. Caruso, M. Antonietti, Chem. Mater. 13 (2001) 3272.
[32] D.T. Mitchell, S.B. Lee, L. Trofin, N. Li, T.K. Nevanen, H. Söderlund, C.R. Martin, J. Am. Chem. Soc. 124 (2002) 11864.
[33] Y. Ono, K. Nakashima, M. Sano, Y. Kanekiyo, K. Inoue, J. Hojo, S. Shinkai, Chem. Commun. (1998) 1477.
[34] G. Gundiah, S. Mukhopadhyay, U.G. Tumkurkar, A. Govindaraj, U. Maitra, C.N.R. Rao, J. Mater. Chem. 13 (2003) 2118.
[35] J.H. Jung, S.-H. Lee, J.S. Yoo, K. Yoshida, T. Shimizu, S. Shinkai, Chem. Eur. J. 9 (2003) 5307.
[36] C.N.R. Rao, B.C. Satishkumar, A. Govindaraj, Chem. Commun. (1997) 1581.
[37] B.C. Satishkumar, A. Govindaraj, E.M. Vogl, L. Basumallick, C.N.R. Rao, J. Mater. Res. 12 (1997) 604.
[38] B.C. Satishkumar, A. Govindaraj, M. Nath, C.N.R. Rao, J. Mater. Chem. 10 (2000) 2115.
[39] S. Naito, M. Ue, S. Sakai, T. Miyao, Chem. Commun. (2005) 1563.
[40] A. Dong, N. Ren, Y. Tang, Y. Wang, Y. Zhang, W. Hua, Z. Gao, J. Am. Chem. Soc. 125 (2003) 4976.
[41] Z. Yang, Y. Xia, R. Mokaya, Adv. Mater. 16 (2004) 727.
[42] R. Yuan, X. Fu, X. Wang, P. Liu, L. Wu, Y. Xu, X. Wang, Z. Wang, Chem. Mater. 18 (2006) 4700.
[43] K.P. de Jong, J.W. Geus, Catal. Rev. Sci. Eng. 42 (2000) 481.
[44] S. Takenaka, Y. Shigeta, E. Tanabe, K. Otsuka, J. Phys. Chem. B 108 (2004) 7656.
[45] S. Yang, X. Chen, M. Kusunoki, K. Yamamoto, H. Iwanaga, S. Motojima, Carbon 4 (2005) 916.
[46] K. Otsuka, S. Kobayashi, S. Takenaka, Appl. Catal. A 210 (2001) 371.
[47] H. Ogihara, M. Sadakane, Y. Nodasaka, W. Ueda, Chem. Mater. 18 (2006) 4981.
[48] J. Jung, Y. Ono, K. Hanabusa, S. Shinkai, J. Am. Chem. Soc. 122 (2000) 5008.
[49] J. Jung, Y. Ono, S. Shinkai, Chem. Eur. J. 6 (2000) 4552.
[50] S. Kobayashi, N. Hamasaki, M. Suzuki, M. Kimura, H. Shirai, K. Hanabusa, J. Am. Chem. Soc. 124 (2002) 6550.
[51] K. Sugiyasu, S. Tamaru, M. Takeuchi, D. Berthier, I. Huc, R. Oda, S. Shinkai, Chem. Commun. (2002) 1212.
[52] J. Jung, K. Yoshida, T. Shimizu, Langmuir 18 (2002) 8724.
[53] S. Motojima, T. Suzuki, Y. Noda, A. Hiraga, H. Iwanaga, T. Hashishin, Y. Hishikawa, S. Yang, X. Chen, Chem. Phys. Lett. 378 (2003) 111.
[54] H. Ogihara, M. Sadakane, Y. Nodasaka, W. Ueda, Chem. Lett. 36 (2007) 258.